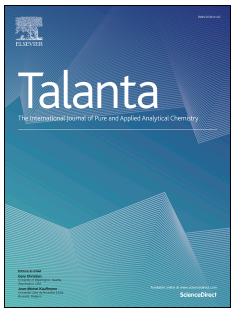

A highly sensitive and specific lateral flow aptasensor for the detection of human osteopontin

Omar Mukama, Wei Wu, Jinghua Wu, Xuewen Lu, Yumei Liu, Yujie Liu, Jiaxin Liu, Lingwen Zeng

PII: S0039-9140(19)31257-3

DOI: https://doi.org/10.1016/j.talanta.2019.120624

Reference: TAL 120624

To appear in: *Talanta*

Received Date: 30 July 2019

Revised Date: 2 December 2019

Accepted Date: 7 December 2019

Please cite this article as: O. Mukama, W. Wu, J. Wu, X. Lu, Y. Liu, Y. Liu, J. Liu, L. Zeng, A highly sensitive and specific lateral flow aptasensor for the detection of human osteopontin, *Talanta* (2020), doi: https://doi.org/10.1016/j.talanta.2019.120624.

Graphical abstract

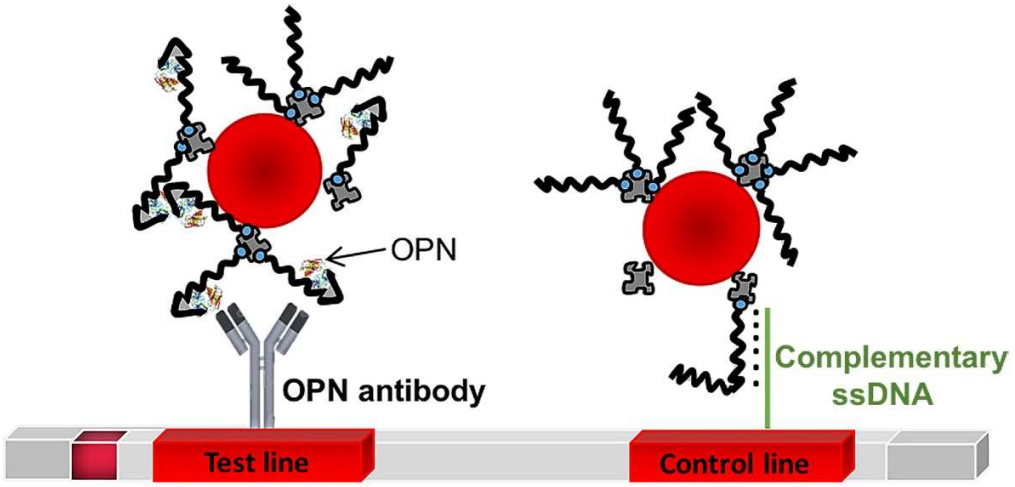

A highly sensitive and specific lateral flow aptasensor for the detection of human osteopontin

Omar Mukama[a,c,f,#], Wei Wu[d,#], Jinghua Wu[b], Xuewen Lu[a], Yumei Liu[b], Yujie Liu[e], Jiaxin Liu[a] and Lingwen Zeng[a,b,*]

[a] Key Laboratory of Regenerative Biology, South China Institute for Stem Cell Biology and Regenerative Medicine, Guangzhou Institutes of Biomedicine and Health, Chinese Academy of Sciences, Guangzhou 510530, China.
[b] School of Food Science and Engineering, Foshan University, Foshan 528231, China.

[c] Department of Applied Biology, College of Science and Technology, University of Rwanda, Avenue de l'armée, P.O. Box: 3900 Kigali-Rwanda.
[d] College of Food Science and Engineering, Qingdao Agricultural University, Qingdao, 266109, China.

[e] Guizhou Provincial Key Laboratory for Regenerative Medicine, Tissue Engineering and Stem Cell Research Center, Department of Immunology, School of Basic Medicine, Guizhou Medical University, Guiyang, China.
[f] University of Chinese Academy of Sciences, 19 Yuquan Road, Shijingshan District, Beijing, 100049, P. R. China.
[#] Co-first authors. These two authors contributed equally to this work.

***** Corresponding Author: zeng6@yahoo.com for Lingwen Zeng.

Abstract

The rapid determination of human osteopontin (OPN) protein, a potential cancer biomarker, holds substantial promise for point-of-care diagnostics and biomedical applications. To date, most reported platforms for OPN detection are apparatus-dependent, time-consuming, and expensive. Herein, we established a lateral flow biosensor (LFB) for OPN detection. A biotinylated aptamer was used for OPN pre-capture from samples, an antibody for OPN was immobilized on the test line for a second specific target identification, and streptavidin-modified gold nanoparticles were sprayed on the conjugation pad for color detection. This LFB achieved as low as 0.1 ng mL^{-1} OPN sensitivity with a good dynamic detection between 10-500 ng mL^{-1} within 5 minutes. Intriguingly, the LFB allowed a qualitative and semi-quantitative detection of OPN in serum at clinically cut-off levels as in cancer patients, and can discriminate OPN from interfering proteins with high specificity. Thus, it is a promising alterative approach for point-of-care OPN screening and detection.

Keywords: Lateral flow assay; Aptasensor; human osteopontin; aptamer; cancer biomarker

1. Introduction

OPN protein is considered as a bridge between bones and blood owing to its localization in tissues and biological fluids [1]. As one of the matricellular proteins, OPN has multiple functional domains regulating various physiological and pathological mechanisms [2]. OPN is involved in several cellular and extracellular processes such as cell adhesion [3], apoptosis, inflammation [4], and diseases [5, 6] especially cancer [2, 7, 8]. Extensive studies have associated OPN with tumor progression, metastasis and aggravation due to its overexpression in the lung [9], breast [10], colon [11, 12], liver [13, 14], oral cavity and solid organ [15]. As a potential cancer biomarker, its targeted suppression has also gained significant attention in prevention and alternation of tumor growth as well as metastasis [14, 16, 17]. Therefore, the rapid determination of OPN level is crucial in biomedicine researches, cancer prognosis, and sepsis [18].

Aptamer-based approaches can target OPN for cancer diagnosis [19] and therapy [17]. Currently, detection methods such as electrochemical aptasensors [19, 20] and Enzyme-linked immunosorbent assay (ELISA) [21] are alternatives to high-performance liquid chromatography (HPLC) [22, 23], surface plasmon resonance (SPR), and spectrometry analytical methods [24, 25], etc. and they are sensitive. However, these assays remain tedious and require complicated procedures and apparatuses. For instance, the electrochemical aptasensor can achieve a good quantification and detection limit of 1.3 ± 0.1 nM for OPN [19]; however, its aptamer immobilization on the electrodes is time-consuming and could be susceptible to interference with other proteins [26]. Moreover, available ELISA-based detection methods are highly sensitive for OPN but are still apparatus-dependent and tedious [21, 27]. Thus, these bottlenecks impede their on-site applications.

LFB is an ideal platform for the rapid detection of various targets, including cancer biomarkers [28-30]. LFB integrates four main parts: sample, conjugate, and absorbent pads,

and a nitrocellulose membrane, which can detect analytes in one-step, rapidly and inexpensively [31] (Fig. 1). In recent years, various methods such as SPR, LFB, electrochemical assays have been combined with nanoparticles and streptavidin (SA)-biotin chemistry to achieve ultrasensitive detection of different targets [32-34]. Besides, based on nanoparticle conjugated to DNA probes and antibody, we have previously developed highly sensitive and specific LFBs for the detection of proteins [35], stem cells and bacteria [36, 37]. However, the direct linkage of aptamers to nanoparticles such as gold nanoparticles (AuNPs) could suffer from steric hindrance, complex fractal aggregation, nucleotide preference, and longer reaction time [38, 39].

Herein, we established a highly sensitive and specific LFB for rapid detection of OPN that relies on a unique property of the combination of single anti-OPN antibody and aptamer. A biotinylated aptamer was used to capture OPN and react rapidly and strongly with AuNPs-SA complex on the conjugate pad. The resulting complex was subsequently captured at the test line by OPN-specific antibody within 5 minutes (Fig. 1). Thus, this developed biosensor for OPN determination provides a great promise in cancer prognosis.

2. Materials and methods

2.1. Materials

Human recombinant OPN protein expressed in HEK 293 cell lines, rabbit polyclonal/monoclonal anti-OPN were purchased from Abcam (Shanghai, China), and anti-rabbit secondary antibody (with HRP) was purchased from Bioroyee (Beijing, China). DNA probe and aptamer were synthesized by Sangon (Shanghai, China). Human serum albumin (HSA), bovine serum albumin (BSA), ovum albumin (OVA), thrombin, trisodium citrate, $HAuCl_4.3H_2O$, and SA were purchased from Sigma–Aldrich (Steinheim, Germany). Absorbent and fiberglass papers and nitrocellulose membranes were purchased from Millipore (Billerica, Massachusetts). Dispenser for antibody, conjugates and probes

immobilization and a paper strip cutter were purchased from Shanghai Kinbio (Shanghai, China). A portable strip reader is from Goldbio Technology Co. (Shanghai, China). All buffer solutions were prepared in our lab. Other reagents of high analytical grade and purity were obtained from other commercial sources.

2.2. Preparation of AuNPs and its conjugates

AuNPs of 15 nm average diameter were prepared by citrate reduction method as previously described [35] with slight modifications. Briefly, 350 mL of 1 mM aqueous gold chloride solution ($HAuCl_4$) was boiled and continuously stirred in a flask, followed by subsequent addition of 3.5 mL of 1% sodium citrate solution. The resulting colorless solution turned to a wine red-like color after 10 minutes boiling. The solution was then cooled at room temperature to form AuNPs and subsequently kept at 4 ◦C until use.

AuNPs–SA conjugate was prepared according to [39] with some modifications. Briefly, 1 mL of the prepared AuNPs solution was collected and concentrated in multiple of two by centrifugation (12000 rpm, 25 min). The resulted AuNPs red pellets were resuspended in 1 mL double distilled water (ddH_2O), and subsequently mixed with 6 µL of K_2CO_3 (0.1 M in ddH_2O) and 10 µL of SA (50 µg mL^{-1} in 10 mM phosphate-buffered saline (PBS). The solution was gently shaken for 3 hours at room temperature and then centrifuged at 12000 rpm, 25 min. The AuNPs-SA complex was resuspended in 100 µL of suspension buffer (0.1% NaN_3, 0.25% Tween-20, 5% BSA, 10% sucrose, and 20 mM Na_3PO_4), and then dispensed on the conjugate pad.

Furthermore, different LFBs were constructed using different concentrations of the AuNPs–SA conjugates by applying 200 ng mL^{-1} of OPN-containing samples [40]. The six-times concentrated AuNPs were used for further experiments because they displayed a stable sensitivity and peak areas and tested, as shown in Fig. S1.

2.3. Construction of lateral flow biosensor

The recognition molecules were immobilized on LFB as previously reported [35] with slight modifications as follows. 30 µL of both rabbit polyclonal anti-OPN (0.7 mg mL^{-1}) and ssDNA capture probe 5'-AAAAAAAAAAAAAAAATAAAAAAAAAAAAAAAAATA A-3' (50 µM) were dispensed on the nitrocellulose membrane of the strip (25 mm in width) using a LFB dispenser to form a test and control zone, respectively. The membrane was then dried at room temperature for 12 h and stored at 4 ◦C until use.

To assemble the detection strip, a fiberglass sample pad (16 mm in width) was immersed in sample pad buffer (1% Triton, 1% BSA, 2% glucose, 50 mM boric acid, pH 8.0), dried and then stored at low-humidity room temperature. The conjugate and absorbent pads (6mm and 17 mm in width, respectively) were used without buffer treatment. As shown in Fig. 1b, all pads were sequentially assembled along the adhesive part of the nitrocellulose membrane with an overlap of 2 mm and then cut into 0.4 cm-wide strips.

2.4. Lateral flow biosensor detection of OPN protein

Prior to sample analysis, biotinylated aptamer (5'–biotin-TGTGTGCGGCACTCCA GTCTGTTACGCCGC**TTTTTTTTTATTTT**-3') were used. This aptamer is linked to biotin at the 5' and extended at the 3'-end with TsATs (bolded), a sequence complementary to the control line of the LFB. To detect OPN by the LFB, an optimized biotinylated aptamer of 20 µL (1µM) was selected from a wide range of concentrations (Fig. S2). The aptamers were diluted in aptamer binding (AB) buffer (10 mM Tris (pH 7.5), 150 mM NaCl, 1 mM $MgCl_2$, 1 mM dithiothreitol (DTT), and 4% glycerol), heat-treated at 95 ◦C for 2 min, and then chilled on ice for 5 min. The aliquots were incubated with 20 µL of different concentrations of purified OPN, OPN-spiked or clinical samples within the AB buffer. The mixtures were then incubated for 30-60 minutes with gentle agitation (500 rpm) at 25 ◦C (Fig. S2). Then, 20 µL of the loading buffer (150 mM NaCl, 20 mM Tris–HCl (pH 8.0)) was mixed with samples prior for subsequent loading to the LFB sample pad. After 5 minutes, the LFB was read using

a portable LFB reader and peak intensities were analyzed using ImageJ (NIH Research Services, US), which provided peak areas for plotting and sensitivity calculation as described previously [41, 42]. Clinical breast cancer patient and normal serum samples were collected from the biological sample bank of Central South University. The normal serum was used to prepare a batch of six different concentrations of OPN-spiked serum and heated serum (50 ◦C, 30 min).

2.5. Statistical analysis

Each result presented is the mean ± SE of the triplicate samples from three independent experiments. Student's T-test was performed using Excel and the differences between samples were considered significant at $*p < 0.05$ or $**p < 0.01$.

3. Results and discussion

3.1. Principle of the OPN lateral flow for detection

AuNPs was conjugated to SA and then dispensed on a conjugate pad. The OPN antibody and an ssDNA probe complementary to one part of the biotin-labeled aptamer sequence were dispensed at the test and control zone of the nitrocellulose membrane, respectively. OPN containing samples incubated with biotinylated aptamer results in aptamer-OPN complex samples (Fig. 1). Upon loading samples on the LFB, the OPN was captured on the LFB by the AuNPs-SA complex on the conjugated pad and subsequently by an anti-OPN antibody immobilized at the test line, generating visible red lines (Fig. 1c). The semi-quantitation was analyzed using a portable strip reader that provided the plotted test lines' intensities responding to the concentration of OPN in purified OPN and OPN-spiked serum. Furthermore, the reproducibility of the assay was assessed by analysis of each sample three times at last twice.

3.2. Sensitivity of the OPN lateral flow biosensor

OPN overexpresses in cancer patients ranging from 100 to 336 (or 495) ng mL^{-1} in serum and plasma [18, 43], and this dramatic increase is related with tumor progression and severity [40, 44]. However, recent reports show that plasma OPN levels is associated with poor cancer prognosis [26]. Therefore, to investigate the sensitivity of the LFB, different concentrations of commercial OPN (0, 0.01, 0.1, 1, 10, 50, 100, 500 ng mL^{-1}), as well as OPN-spiked serum were subjected to the LFB. As shown in Fig. 2a, no positive result was observed in the controls. The purified OPN higher than 0.01 ng mL^{-1} displayed a red test line optical response on the LFB within 5 minutes. The test line directly correlated with the concentration of OPN with a detection as low as 0.1 ng mL^{-1} (Fig. 2b). Consistently, the band intensities of the test lines increased with the concentration of OPN with linear relationship between peak areas and OPN concentration in tested range of 0-500 ng mL^{-1} and the R^2 value was 0.89 (Fig. 2c). The calculated mean peak areas from imageJ of each test line loaded with 3 controls (0 ng mL^{-1}) was 7.3±0.5, which was used to calculate the sensitivity according to LOD = Mean (M) + 3* standard deviation (SD) [41, 42]. The calculated LOD value of 8.8 ng mL^{-1} was then taken into the equation y= 332.74x - 780.87 to obtain an approximate LOD concentration of 11.1 ng mL^{-1}. Notably, the sensitivity of the LFB was confirmed by SDS-PAGE, which was less sensitive but showed a similar trend of band intensity that changed with the loaded concentrations of OPN (Fig. S3).

The sensitivity of our biosensor was confirmed using serum spiked with different concentrations of OPN (0, 5, 10, 50, 100, 500 ng mL^{-1}). As shown in Fig. 3a, this LFB detected as low as 10 ng mL^{-1} in spiked serum with visible detection bands from 10-500 ng mL^{-1}, and the corresponding peak areas are shown in Fig. 3b. The LOD was calculated as previously described, which provided an estimated LOD concentration of 10.3 ng mL^{-1} according to the equation y= 571.01x - 893.01. This sensitivity was obtained within 5 minutes, and is much faster than previously reported methods for OPN detection [20, 45].

Though less than 5 ng mL^{-1} OPN were not recovered, the LFB met the cut-off values for OPN biomarker-based cancer detection [26, 44, 46]. We furthermore validated the assay by conventional ELISA according to the antibodies' source[1] using the serum samples spiked with OPN. As expected, the absorbance increased with increasing the amount of OPN in spiked serum samples (Fig. 3c), and the trend was similar to that of the LFB test lines (Fig. 3a). The resulting plots of both our LFB and ELISA showed a linear relationship between plots and the spiked OPN concentrations of 0.91 and 0.94, respectively. Although the conventional ELISA showed higher sensitivity, our method met the cut-off level with a much fast performance (within 5 minutes) than ELISA (>2 hours) and other methods for OPN detection [21].

Finally, our essay was validated using clinical breast cancer serum and normal samples. As shown in Fig. 3 d, e; no detectable test line was observed from normal people, while a visible red line was observed at the test line in a breast cancer patient. This activity was also confirmed using ELISA, which showed a similar trend as our biosensor but slighly increased signals in the normal sample (Fig. S4). This robust performance of our LFB could be attributed to the stable reaction between AuNPs and biotinylated aptamer through SA-biotin linkage on the conjugate pad. Distinct from our previous finding [35], this LFB was leveraged to use an inbuilt conjugate pad containing AuNPs-SA complex, allowing direct loading of samples without pretreatment with AuNPs-biotinylated aptamer complex. Thus, this method does not require the storage of AuNPs conjugates, which could cause aggregation or dissociation of the complex. Moreover, this linkage is stable and doesn't depend on nucleotide base contents of affinity probes, as for direct linkage of DNA probes to AuNPs have more affinity to adenine and cytosine than thymine [47]. Furthermore, apart from fluorescent dyes, the usage of AuNPs enabled the visualization of the results by naked eye. Nevertheless, further assays from various and additional cancer patient's serum samples

would be indispensable to validate the proposed LFB. Thus, it may be useful for rapid and reliable on-site diagnosis of other biomarkers.

3.3. Specificity of the OPN lateral flow biosensor

This LFB showed high specificity towards various interfering compounds, including OVA, BSA, HSA, thrombin, and heated serum. The interference test was performed using 200 µg of interfering proteins dissolved in PBS/serum. The red test line was only observed in the OPN spiked solution, rather than in the non-target proteins and heated serum (Fig. 4a). Consistently, a detectable peak was only observed in the OPN containing solutions (Fig. 4b).

As OPN is found in various complex body fluids such as blood [48, 49], we furthermore investigated the interference of other components using OPN spiked with the same interfering proteins in serum. As shown in Fig. 5a, the red test line was observed in all OPN-interferants spiked serum, and the corresponding peak areas test lines signals are shown in Fig. 5c. The results suggest that only OPN was pre-captured by the aptamer, and visually detected after binding to the OPN antibody on the LFB test line. This LFB performance showed no observable interference of serum components on the test line, thus discounting steric hindrance as found in electrochemical aptasensors for OPN [19]. The specificity of this LFB can be attributed to two main reasons: one is the AuNPs-SA complex that captures OPN-Aptamer complex through biotin-SA reaction within a short time of conjugation, and another factor could be the OPN antibody specificity immobilized on the test line. Thus, OPN is captured by both aptamers and its antibody, offering a dual specificity.

Noteworthy, OPN possesses multiple sites of post-translational modification and cleavage [50]. OPN is prone to be cleaved, in particular, by thrombin, which is detected in high level (360-611 nM) in cancer patients with different tumor sites and stages; and monitored patients undergoing treatment (surgery, chemotherapy, radiotherapy) presented lower concentrations [51]. Thus, patients with cancer are at high risk of developing venous thromboembolism (an

increase of thrombin), with a hazard ratio of the continuous peak thrombin are given per 100 nM increase. Interestingly, the biosensor was challenged with additional concentrations of thrombin in OPN/serum and the interferant proteins, retained the actual activity (Fig. 5a). However, weak test line signals were observed at higher concentrations of thrombin (Fig. 5b, c). The specificity of the LFB was maintained because the used anti-OPN targets peptide corresponding to human OPN amino acid ^{170}CKSKKFRRPDIQYPD^{183} rather than at thrombin cleavage site ^{160}R and ^{169}S. Of main interest, thrombin couldn't interfere significantly with the OPN aptamer owing to its specific targeting of the OPN N-terminal [19]. Thus, this assay could be important for sepsis, intensive care unit setting, and emergency departments as it is quick, easy, and reliable for osteopontin quantitation.

4. Conclusion

In conclusion, a simple, rapid, sensitive, and highly specific biosensor was developed for human osteopontin (OPN) detection. The biosensor successfully detected both purified OPN and OPN-spiked complex samples such as serum. Compared with other available OPN methods such as ELISA [21] and electrochemical biosensor [19]. It is reasonable to conclude that this biosensor is of low cost, straightforward, simple to use, and provides a fast-visual detection response within 5 min. In addition, it is highly specific given that no background was obtained on the test line in the presence of interfering proteins, which can be explained by the pre-binding of aptamer on the target OPN and the specific OPN antibody fixed on the test line. Our biosensor can be employed for qualitative and semi-quantitative detection of OPN in simple and complex samples such as serum. More importantly, the developed method can be used to detect rapidly and conveniently several other biomarkers by replacing target recognition elements (antibody, aptamer, etc.).

Acknowledgments

This work was supported by the strategic Cooperation of the Chinese Academy of Sciences-The World Academy of Sciences and National Natural Science Foundation of China (31671933) and Guangdong Province Fund (Y55X011121). We thank the biological sample bank of Central South University for providing human serum.

Declaration of interest

None

References

[1] D.N. Haylock, S.K. Nilsson, Osteopontin: a bridge between bone and blood, British Journal of Haematology 134(5) (2006) 467-474.
[2] R. Das, G.H. Mahabeleshwar, G.C. Kundu, Osteopontin stimulates cell motility and nuclear factor kappaB-mediated secretion of urokinase type plasminogen activator through phosphatidylinositol 3-kinase/Akt signaling pathways in breast cancer cells, The Journal of biological chemistry 278(31) (2003) 28593-606.
[3] F.P. Reinholt, K. Hultenby, A. Oldberg, D. Heinegård, Osteopontin--a possible anchor of osteoclasts to bone, Proc. Natl. Acad. Sci. U. S. A. 87(12) (1990) 4473-4475.
[4] F. Takahashi, K. Takahashi, K. Shimizu, R. Cui, N. Tada, H. Takahashi, S. Soma, M. Yoshioka, Y. Fukuchi, Osteopontin is strongly expressed by alveolar macrophages in the lungs of acute respiratory distress syndrome, Lung 182(3) (2004) 173-85.
[5] A. Strom, A. Franzen, C. Wangnerud, A.K. Knutsson, D. Heinegard, A. Hultgardh-Nilsson, Altered vascular remodeling in osteopontin-deficient atherosclerotic mice, Journal of vascular research 41(4) (2004) 314-22.
[6] D.S. Bautista, J. Denstedt, A.F. Chambers, J.F. Harris, Low-molecular-weight variants of osteopontin generated by serine proteinases in urine of patients with kidney stones, Journal of cellular biochemistry 61(3) (1996) 402-9.
[7] H. Teramoto, M.D. Castellone, R.L. Malek, N. Letwin, B. Frank, J.S. Gutkind, N.H. Lee, Autocrine activation of an osteopontin-CD44-Rac pathway enhances invasion and transformation by H-RasV12, Oncogene 24(3) (2005) 489-501.
[8] P.Y. Wai, P.C. Kuo, The role of Osteopontin in tumor metastasis, The Journal of surgical research 121(2) (2004) 228-41.
[9] Z. Hu, D. Lin, J. Yuan, T. Xiao, H. Zhang, W. Sun, N. Han, Y. Ma, X. Di, M. Gao, J. Ma, J. Zhang, S. Cheng, Y. Gao, Overexpression of osteopontin is associated with more aggressive phenotypes in human non-small cell lung cancer, Clinical cancer research : an official journal of the American Association for Cancer Research 11(13) (2005) 4646-52.
[10] V.H. Bramwell, A.B. Tuck, J.A. Chapman, P.H. Anborgh, C.O. Postenka, W. Al-Katib, L.E. Shepherd, L. Han, C.F. Wilson, K.I. Pritchard, M.N. Pollak, A.F. Chambers, Assessment of osteopontin in early breast cancer: correlative study in a randomised clinical trial, Breast cancer research : BCR 16(1) (2014) R8.
[11] Y. He, K. Zeng, S. Zhang, A.S. Gurung, M. Baloda, X. Zhang, G. Liu, Visual detection of gene mutations based on isothermal strand-displacement polymerase reaction and lateral flow strip, Biosensors and Bioelectronics 31(1) (2012) 310-315.
[12] M. Zhao, F. Liang, B. Zhang, W. Yan, J. Zhang, The impact of osteopontin on prognosis and clinicopathology of colorectal cancer patients: a systematic meta-analysis, Scientific reports 5 (2015) 12713-12713.

[13] M. Gotoh, M. Sakamoto, K. Kanetaka, M. Chuuma, S. Hirohashi, Overexpression of osteopontin in hepatocellular carcinoma, Pathology international 52(1) (2002) 19-24.
[14] D. Lorena, I.A. Darby, A.P. Gadeau, L.L. Leen, S. Rittling, L.C. Porto, J. Rosenbaum, A. Desmouliere, Osteopontin expression in normal and fibrotic liver. altered liver healing in osteopontin-deficient mice, Journal of hepatology 44(2) (2006) 383-90.
[15] H. Zhao, Q. Chen, A. Alam, J. Cui, K.C. Suen, A.P. Soo, S. Eguchi, J. Gu, D. Ma, The role of osteopontin in the progression of solid organ tumour, Cell Death & Disease 9(3) (2018) 356.
[16] S.R. Rittling, P.L. Wejse, K. Yagiz, G.A. Warot, T. Hui, Suppression of tumour growth by orally administered osteopontin is accompanied by alterations in tumour blood vessels, British Journal Of Cancer 110 (2014) 1269.
[17] Z. Mi, H. Guo, M.B. Russell, Y. Liu, B.A. Sullenger, P.C. Kuo, RNA Aptamer Blockade of Osteopontin Inhibits Growth and Metastasis of MDA-MB231 Breast Cancer Cells, Molecular Therapy 17(1) (2009) 153-161.
[18] R. Vaschetto, S. Nicola, C. Olivieri, E. Boggio, F. Piccolella, R. Mesturini, F. Damnotti, D. Colombo, P. Navalesi, F. Della Corte, U. Dianzani, A. Chiocchetti, Serum levels of osteopontin are increased in SIRS and sepsis, Intensive Care Medicine 34(12) (2008) 2176-2184.
[19] S.G. Meirinho, L.G. Dias, A.M. Peres, L.R. Rodrigues, Electrochemical aptasensor for human osteopontin detection using a DNA aptamer selected by SELEX, Analytica Chimica Acta 987 (2017) 25-37.
[20] S.G. Meirinho, L.G. Dias, A.M. Peres, L.R. Rodrigues, Development of an Electrochemical Aptasensor for the Detection of Human Osteopontin, Procedia Engineering 87 (2014) 316-319.
[21] D. Chakraborty, T.S. Viveka, K. Arvind, V. Shyamsundar, M. Kanchan, S.A. Alex, N. Chandrasekaran, R. Vijayalakshmi, A. Mukherjee, A facile gold nanoparticle–based ELISA system for detection of osteopontin in saliva: Towards oral cancer diagnostics, Clinica Chimica Acta 477 (2018) 166-172.
[22] F.A. Saad, E. Salih, M.J. Glimcher, Identification of osteopontin phosphorylation sites involved in bone remodeling and inhibition of pathological calcification, Journal of cellular biochemistry 103(3) (2008) 852-856.
[23] S. Lenton, M. Grimaldo, F. Roosen-Runge, F. Schreiber, T. Nylander, R. Clegg, C. Holt, M. Hartlein, V. Garcia Sakai, T. Seydel, S.C. Marujo Teixeira, Effect of Phosphorylation on a Human-like Osteopontin Peptide, Biophysical journal 112(8) (2017) 1586-1596.
[24] B. Christensen, L. Schack, E. Kläning, E.S. Sørensen, Osteopontin is cleaved at multiple sites close to its integrin-binding motifs in milk and is a novel substrate for plasmin and cathepsin D, The Journal of biological chemistry 285(11) (2010) 7929-7937.
[25] H. Chen, Q. Mei, S. Jia, K. Koh, K. Wang, X. Liu, High specific detection of osteopontin using a three-dimensional copolymer layer support based on electrochemical impedance spectroscopy, Analyst 139(18) (2014) 4476-4481.
[26] S.S. El-Din Bessa, N.M. Elwan, G.A.M. Suliman, S.H. El-Shourbagy, Clinical Significance of Plasma Osteopontin Level in Egyptian Patients with Hepatitis C Virus-related Hepatocellular Carcinoma, Archives of Medical Research 41(7) (2010) 541-547.
[27] V.H.C. Bramwell, A.B. Tuck, J.-A.W. Chapman, P.H. Anborgh, C.O. Postenka, W. Al-Katib, L.E. Shepherd, L. Han, C.F. Wilson, K.I. Pritchard, M.N. Pollak, A.F. Chambers, Assessment of osteopontin in early breast cancer: correlative study in a randomised clinical trial, Breast cancer research : BCR 16(1) (2014) R8-R8.
[28] K. Baryeh, S. Takalkar, M. Lund, G. Liu, Development of quantitative immunochromatographic assay for rapid and sensitive detection of carbohydrate antigen 19-9

(CA 19-9) in human plasma, Journal of Pharmaceutical and Biomedical Analysis 146 (2017) 285-291.
[29] Y. Huang, Y. Wen, K. Baryeh, S. Takalkar, M. Lund, X. Zhang, G. Liu, Lateral flow assay for carbohydrate antigen 19–9 in whole blood by using magnetized carbon nanotubes, Microchimica Acta 184(11) (2017) 4287-4294.
[30] O. Mukama, J.P. Sinumvayo, M. Shamoon, M. Shoaib, H. Mushimiyimana, W. Safdar, L. Bemena, P. Rwibasira, S. Mugisha, Z. Wang, An Update on Aptamer-Based Multiplex System Approaches for the Detection of Common Foodborne Pathogens, Food Analytical Methods 10(7) (2017) 2549-2565.
[31] M. Sajid, A.-N. Kawde, M. Daud, Designs, formats and applications of lateral flow assay: A literature review, Journal of Saudi Chemical Society 19(6) (2015) 689-705.
[32] L. Guo, J.A. Jackman, H.-H. Yang, P. Chen, N.-J. Cho, D.-H. Kim, Strategies for enhancing the sensitivity of plasmonic nanosensors, Nano Today 10(2) (2015) 213-239.
[33] H.-S. Kim, Y.-J. Kim, J.-W. Chon, D.-H. Kim, J.-H. Yim, H. Kim, K.-H. Seo, Two-stage label-free aptasensing platform for rapid detection of Cronobacter sakazakii in powdered infant formula, Sensors and Actuators B: Chemical 239 (2017) 94-99.
[34] S.Y. Oh, N.S. Heo, S. Shukla, H.-J. Cho, A.T.E. Vilian, J. Kim, S.Y. Lee, Y.-K. Han, S.M. Yoo, Y.S. Huh, Development of gold nanoparticle-aptamer-based LSPR sensing chips for the rapid detection of Salmonella typhimurium in pork meat, Scientific reports 7(1) (2017) 10130-10130.
[35] Z. Fang, C. Ge, W. Zhang, P. Lie, L. Zeng, A lateral flow biosensor for rapid detection of DNA-binding protein c-jun, Biosensors and Bioelectronics 27(1) (2011) 192-196.
[36] W. Wu, S. Zhao, Y. Mao, Z. Fang, X. Lu, L. Zeng, A sensitive lateral flow biosensor for Escherichia coli O157:H7 detection based on aptamer mediated strand displacement amplification, Analytica chimica acta 861 (2015) 62-68.
[37] Z. Fang, W. Wu, X. Lu, L. Zeng, Lateral flow biosensor for DNA extraction-free detection of salmonella based on aptamer mediated strand displacement amplification, Biosensors and Bioelectronics 56 (2014) 192-197.
[38] P. Kalra, A. Dhiman, W.C. Cho, J.G. Bruno, T.K. Sharma, Simple Methods and Rational Design for Enhancing Aptamer Sensitivity and Specificity, Frontiers in Molecular Biosciences 5(41) (2018).
[39] R. D'Agata, P. Palladino, G. Spoto, Streptavidin-coated gold nanoparticles: critical role of oligonucleotides on stability and fractal aggregation, Beilstein journal of nanotechnology 8 (2017) 1-11.
[40] Salem, Clinical Significance of Plasma Osteopontin Level as a Biomarker of Hepatocellular Carcinoma, 2013.
[41] B. Fang, S. Hu, C. Wang, M. Yuan, Z. Huang, K. Xing, D. Liu, J. Peng, W. Lai, Lateral flow immunoassays combining enrichment and colorimetry-fluorescence quantitative detection of sulfamethazine in milk based on trifunctional magnetic nanobeads, Food Control 98 (2019) 268-273.
[42] B.J. Toley, I. Covelli, Y. Belousov, S. Ramachandran, E. Kline, N. Scarr, N. Vermeulen, W. Mahoney, B.R. Lutz, P. Yager, Isothermal strand displacement amplification (iSDA): a rapid and sensitive method of nucleic acid amplification for point-of-care diagnosis, Analyst 140(22) (2015) 7540-9.
[43] M. Bache, M. Kappler, H. Wichmann, S. Rot, A. Hahnel, T. Greither, H.M. Said, M. Kotzsch, P. Würl, H. Taubert, D. Vordermark, Elevated tumor and serum levels of the hypoxia-associated protein osteopontin are associated with prognosis for soft tissue sarcoma patients, BMC Cancer 10(1) (2010) 132.

[44] A. Simão, J. Madaleno, N. Silva, F. Rodrigues, P. Caseiro, J.N. Costa, A. Carvalho, Plasma osteopontin is a biomarker for the severity of alcoholic liver cirrhosis, not for hepatocellular carcinoma screening, BMC gastroenterology 15 (2015) 73-73.
[45] D. Chakraborty, T.S. Viveka, K. Arvind, V. Shyamsundar, M. Kanchan, S.A. Alex, N. Chandrasekaran, R. Vijayalakshmi, A. Mukherjee, A facile gold nanoparticle-based ELISA system for detection of osteopontin in saliva: Towards oral cancer diagnostics, Clinica chimica acta; international journal of clinical chemistry 477 (2018) 166-172.
[46] L. Zhao, Y. Wang, N. Qu, C. Huang, L. Chen, Significance of Plasma Osteopontin Levels in Patients with Bladder Urothelial Carcinomas, Molecular Diagnosis & Therapy 16(5) (2012) 311-316.
[47] P. Kalra, A. Dhiman, W.C. Cho, J.G. Bruno, T.K. Sharma, Simple Methods and Rational Design for Enhancing Aptamer Sensitivity and Specificity, Frontiers in molecular biosciences 5 (2018) 41-41.
[48] N. Razmi, B. Baradaran, M. Hejazi, M. Hasanzadeh, J. Mosafer, A. Mokhtarzadeh, M. de la Guardia, Recent advances on aptamer-based biosensors to detection of platelet-derived growth factor, Biosensors and Bioelectronics 113 (2018) 58-71.
[49] P.-L. Chang, L. Harkins, Y.-H. Hsieh, P. Hicks, K. Sappayatosok, S. Yodsanga, S. Swasdison, A.F. Chambers, C.A. Elmets, K.-J. Ho, Osteopontin expression in normal skin and non-melanoma skin tumors, The journal of histochemistry and cytochemistry : official journal of the Histochemistry Society 56(1) (2008) 57-66.
[50] S. Razzouk, J.C. Brunn, C. Qin, C.E. Tye, H.A. Goldberg, W.T. Butler, Osteopontin posttranslational modifications, possibly phosphorylation, are required for in vitro bone resorption but not osteoclast adhesion, Bone 30(1) (2002) 40-47.
[51] C. Ay, D. Dunkler, R. Simanek, J. Thaler, S. Koder, C. Marosi, C. Zielinski, I. Pabinger, Prediction of Venous Thromboembolism in Patients With Cancer by Measuring Thrombin Generation: Results From the Vienna Cancer and Thrombosis Study, Journal of Clinical Oncology 29(15) (2011) 2099-2103.

Figures

Fig. 1. Illustrative scheme of the OPN LFB. **(**a) The biotinylated aptamer was incubated with OPN-containing samples to obtain a stable aptamer-OPN complex and applied on the sample pad (reversed arrow). (b) The OPN LFB assembly with AuNPs-SA on the conjugate pad, immobilized OPN antibody and a probe complementary to the aptamer on the nitrocellulose membrane. (c) OPN-aptamer complex containing samples subjected to the LFB sample pad flow and react with AuNPs-SA on the conjugate pad, then subsequently captured by the anti-OPN antibody at the test line. Then, the excess biotinylated OPN aptamers are captured by the partially complementary ssDNA probes immobilized on the control line.

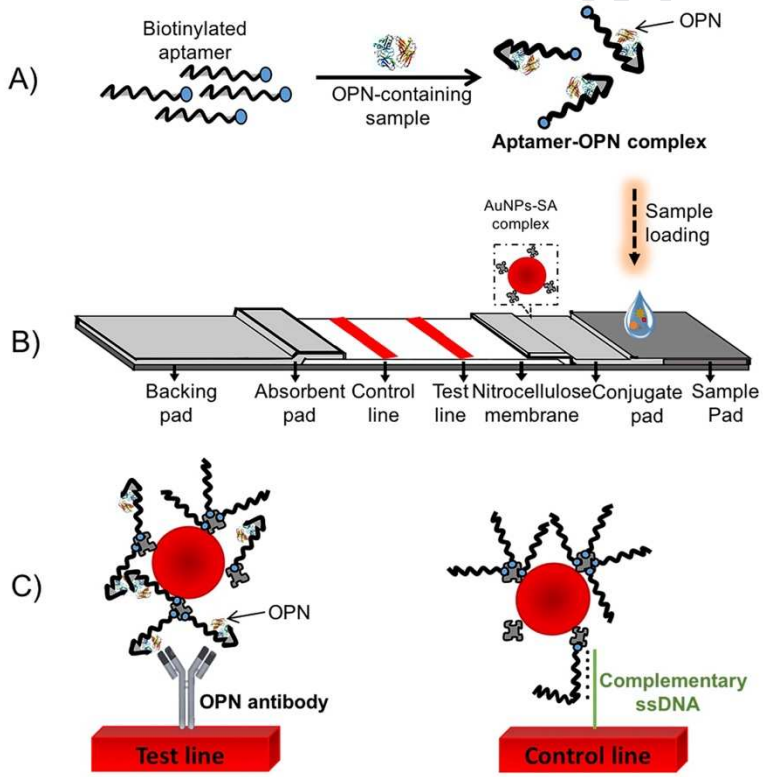

Fig. 2. (ab) Side-by-side analysis of LFB images (left) and corresponding intensities (right) loaded with buffer and different concentrations of purified OPN (0, 0.1, 1, 10, 50, 100, 500 ng mL^{-1}). (c) LFB portable reader peaks corresponding to the LFB test line intensities at different concentrations of purified OPN. The peak areas of the LFB test lines of the purified OPN in (a) were calculated and plotted. Data presented are the mean ± SE of three independent samples. (*$p < 0.05$, **$p < 0.01$; n=3).

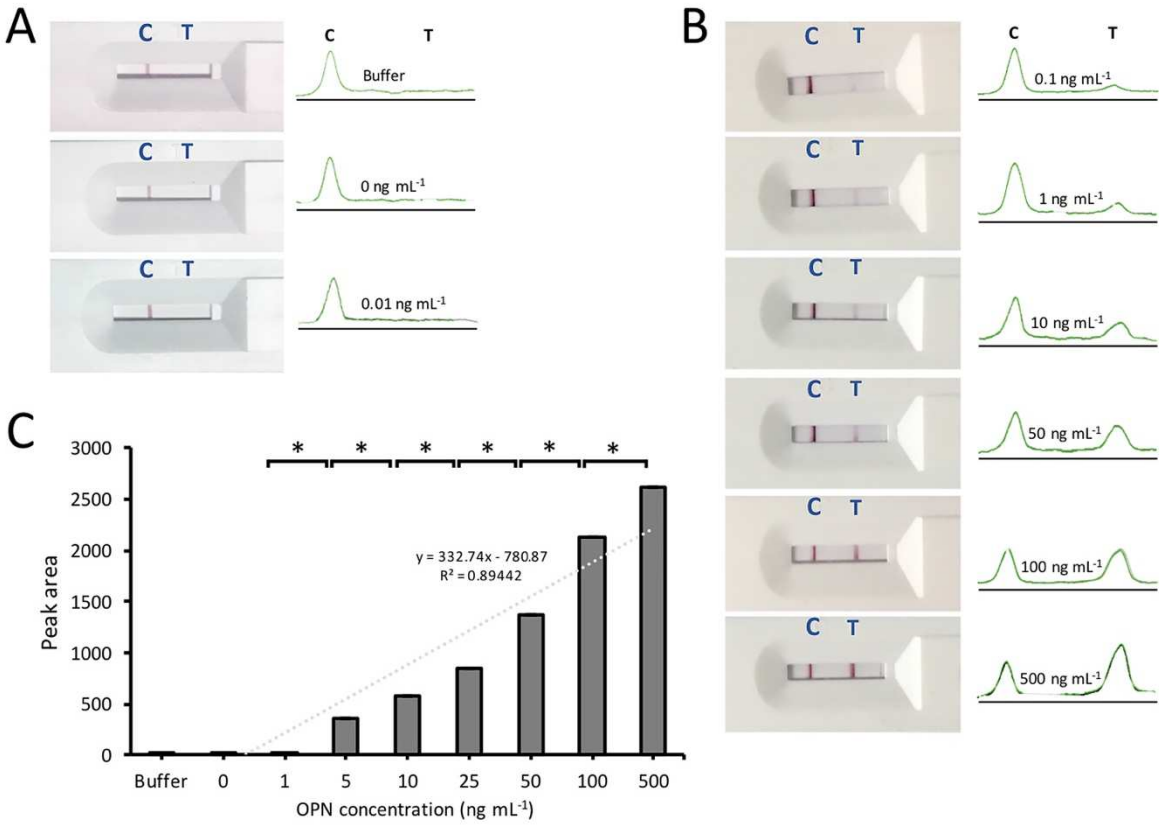

Fig. 3. Biosensor sensitivity for OPN concentrations spiked in serum and clinical samples. (a) From top down is the gradual increase of the test line intensity respective to the applied concentrations of OPN and clinical samples. (b) The peak areas of the LFB test lines in (a) corresponding to the concentrations of OPN spiked in the serum. (c) Conventional ELISA detection for the purified OPN (standard OPN) and OPN-spiked serum. (d) Photo images (left) and corresponding intensities (right) of the biosensors loaded with clinical serum. (e) The peak areas of the LFB test lines in (d) corresponding to serum samples of breast cancer patient, normal people and buffer (0). Data presented are the mean ± SE of three independent samples. (*$p < 0.05$, **$p < 0.01$; n=3).

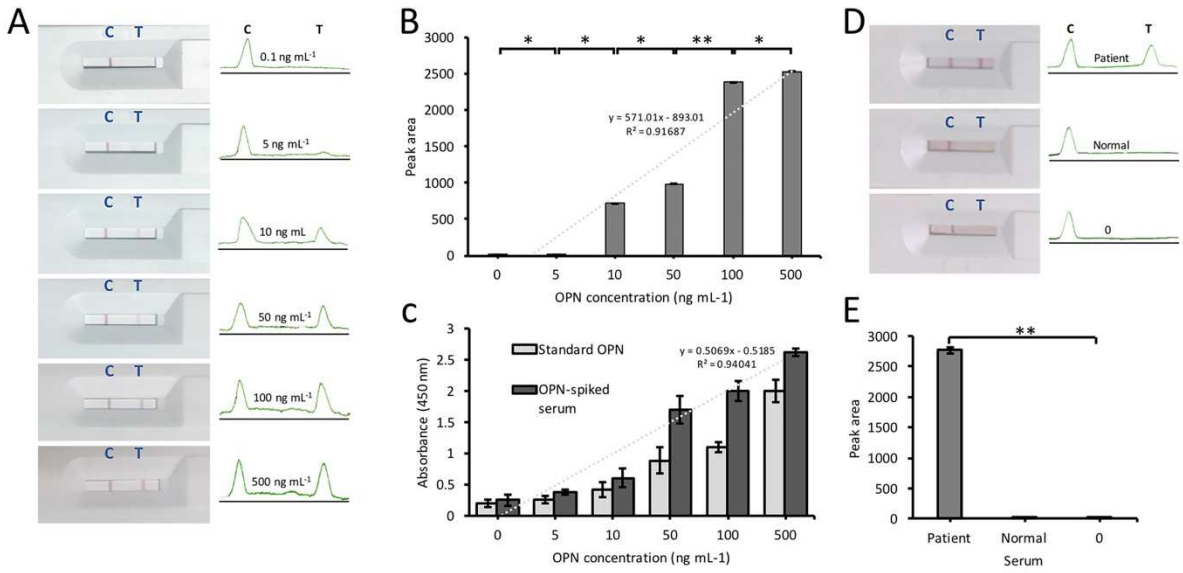

Fig. 4. (a) Side-by-side analysis of LFB images loaded with interfering proteins such as OVA, BSA, HSA, thrombin, serum dissolved in PBS and heated serum containing 200 ng mL^{-1} purified OPN solutions. (b) Portable LFB reader peak intensities corresponding to different concentrations of interfering proteins in PBS and purified OPN on the test line. (c) The peak areas of the LFB test lines in (a) were measured and plotted. The absence of OPN and usage of heated serum generated neither test line nor a peak. Data presented are the mean ± SE of three independent samples. (*$p < 0.05$, **$p < 0.01$; n=3).

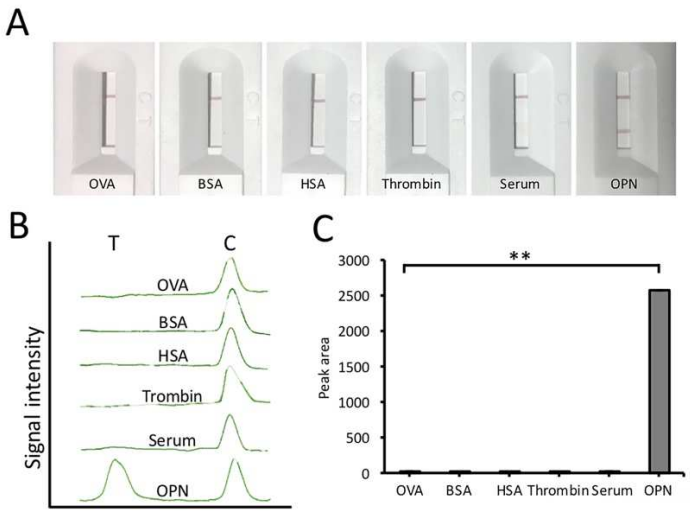

Fig. 5. (a) The reaction mixture of 200 ng mL^{-1} purified OPN solutions mixed with interfering proteins such as OVA, BSA, HSA, and thrombin within the heated serum. (b) Portable LFB reader peaks on the test line corresponding to detectable OPN in the presence of interferants. (c) The peak areas of the LFB test lines in (a) were measured and plotted. Data presented are the mean ± SE of three independent samples. (*$p < 0.05$, **$p < 0.01$; n=3).

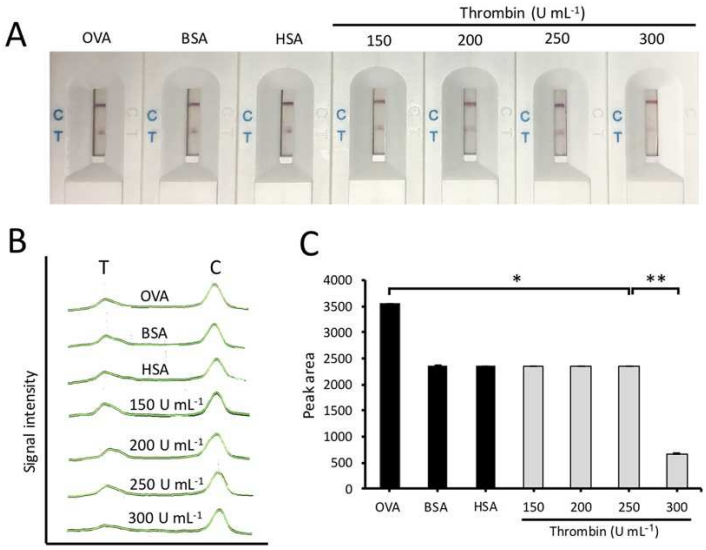

Highlights

1. Specific aptamer and antibody for Osteopontin was used in this study;

2. The limit of detection is as low as 10 ng mL^{-1};

3. Results can be observed by naked eyes in less than an hour;

4. The lateral flow strip can be used in biomedicine research and cancer prognosis.

Declaration of interests

☑ The authors declare that they have no known competing financial interests or personal relationships that could have appeared to influence the work reported in this paper.

☐ The authors declare the following financial interests/personal relationships which may be considered as potential competing interests:

Authors agreement

All authors declare that they have read this manuscript, accept its content and are aware of its submission to Talanta.

Authors statement

O.M and L.W.Z contributed to the concept and biosensor design, fabrication and manuscript preparation. O.M, W.W, YM.L, and J.W performed the experiments and data curation. YJ.L, J.L, and X.L gave experimental support (e.g. method validation) and manuscript proof-reading. L.W.Z directed and supervised this work.